Transient Characteristics and Sites of Pre-Breakdown in Spark Conditioning for High-voltage Vacuum Interrupter under Power Frequency Voltage

Hui Ma | Yu Du | Jingyu Shen | Yuanzhao Li | Yulong Gao | Zhiyuan Liu | Jianhua Wang | Yingsan Geng

State Key Laboratory of Electrical Insulation and Power Equipment, Xi'an Jiaotong University, Xi'an 710049, People's Republic of China

Correspondence
Hui Ma, State Key Laboratory of Electrical Insulation and Power Equipment, Xi'an Jiaotong University, Xi'an 710049, People's Republic of China.
Email: mhxjtu@xjtu.edu.cn

Funding information
National Key Research and Development Program of China,
Grant/Award Number: 2022YFB2403700;
National Natural Science Foundation of China,
Grant/Award Number: 51937009;

Conflict of Interest
No conflict of interest exits in the submission of this manuscript, and manuscript is approved by all authors for publication.

Permission to reproduce materials from other sources
None.

Data Availability
The data that support the findings of this study are available from the corresponding author upon reasonable request.

Abstract

The spark conditioning has become a key process to improve the breakdown voltage for high-voltage vacuum interrupters. The objective of this paper is to determine the transient characteristics and sites of the pre-breakdown (pre-BD) in the spark conditioning under power frequency voltage (PFV) in vacuum. A multi-angle optical path system was built to record the arc of pre-BD at two viewing angles by one camera, realizing the determination of the pre-BD sites in spark conditioning. The recording rate of high-speed camera was 580,000 frames/s. The experimental results indicate that, in the spark conditioning under PFV, the pre-BDs continuously occurred at a random moment. Within several half-waves, the number of the pre-BDs could reach dozens of times, which was the key for the treatment of the electrode surface in conditioning. Under the application of PFV, the single pre-BD occurred at a random moment, in which would last for several microseconds and the peak value of the current would reach several amperes. Moreover, the pre-BD sites randomly distributed in the surface of the electrode and almost covered the whole surface of the electrode. The number of the pre-BDs in edge region of the electrode tent to be more. The pre-BDs took place independently in both time and space, in which there should be no effect between each other of two sequential pre-BDs.

1 | INTRODUCTION

With rapid development of vacuum circuit breakers (VCBs) to high voltage power systems of 110 kV and over, the insulation performance has become a great challenge for VCBs [1-3]. Vacuum interrupter, as the core component, plays a decisive role in the electric strength of the VCBs [3, 4]. Especially in high-voltage systems, it is important to ensure and improve the reliability of the electric strength of vacuum interrupter.

Conditioning process has been considered an effective method for the improvement of the dielectric strength of high-voltage vacuum interrupters [4-8]. Conditioning process can melt the partial materials and reduce the particles and defects in electrode surface. This change in the electrode surface can strongly improve the breakdown(BD) voltage and reduce the BD probability of vacuum gaps. Spark conditioning is one of the conditioning methods, in which the electrodes are conditioned by high-voltage sources, mainly including the power frequency voltage (PFV), the lightning impulse voltage (LIV) and other high frequency impulse voltages.

Recently, many researches on the characteristics of the spark conditioning under the PFV and the LIV have been done based on the basic theories and experiments. Cross *et al.*[9] experimentally pointed out that the adsorbed gas removal was the cause for the effect of the conditioning in vacuum BD. Shioiri *et al.* [10] and Okubo *et al.* [11] indicated that the electrode area might determine the duration of conditioning process and the BD voltages depended on electrode area. Kato *et al.*[4, 12] and Schneider *et al.* [13] investigated the electrode conditioning mechanism in vacuum and found that the BD field strength and the number of voltage applications required for conditioning were much different depending on the voltage application procedures. Kojima *et al.* [14-16] investigated the BD characteristics for spark conditioning in vacuum under various non-uniform electric fields of LIV and with different anode materials. They discussed the BD mechanism in terms of BD arising from anode heating or cathode

heating, and proposed the optimum BD charge for the maximum dielectric strength in spark conditioning in vacuum [16]. Erven *et al.* [6] investigated the vacuum insulation under 60 Hz PFV during the conditioning process and proposed the pre-BD phenomena in the inter-electrode gap. They found protrusion development on the electrode surfaces were different from those under the direct current (DC) conditioning. Balachandra *et al.* [17] indicated that, for stainless steel, copper and aluminum anodes, the temperature of hot spots can reach the melting point for reasonable values of the field intensification factor for vacuum gaps, subjected to 50 Hz AC excitations. Yang *et al.* [18] found that the shunt capacitors of vacuum interrupters could make the BD sites cover the entire contact surface very evenly, under PFV conditioning. Latham *et al.* [19-21] investigated the pre-BD sites distributions on a rounded shaped cathode through a transparent anode. Du and Ma *et al.* [22, 23] experimentally determined the distribution of the BD sites in conditioning progress under the LIV in vacuum. However, the transient characteristics and mechanism of the pre-BD in spark conditioning process under the PFV in vacuum is not clearly yet.

The objective of this paper is to determine the transient characteristics and sites of the pre-BD in the spark conditioning under the PFV in vacuum. In Section 2, besides the experimental systems and the test specimen, a multi-angle optical path system for the determination of pre-BD sites in spark conditioning for vacuum interrupter was introduced in detail. In Section 3, the transient characteristics and the sites of the pre-BDs in the spark conditioning under PFV were determined experimentally. The results also reveal the sequential relationship of the pre-BD sites. The results in this paper are quite significant to understand the physical mechanism in the spark conditioning and helpfully to improve the BD voltage of vacuum interrupters.

2 | EXPERIMENTAL SETUP

2.1 | Test Specimen

Fig. 1 displays the schematic configuration of the experimental vacuum interrupters. A glass tube of the vacuum interrupter without central shield made the recording of the BD easily. The diameter of the plane-plane electrodes was 18 mm. The material of the electrodes was CuCr50 (50%Cr), with a thickness of 5 mm. A chamfering radius was set at the electrode edge of 1 mm. The diameter of the conductive rod was 12 mm. In experiments, length of the electrode gap was set at 2.0 mm.

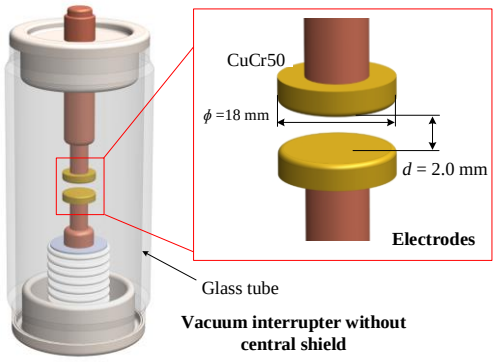

FIGURE 1 Structural parameter of the experimental vacuum interrupter.

2.2 | Experimental System Setup

Fig. 2 shows the schematic of the experimental system setup in the spark conditioning under the PFV. The PFV (50Hz) was generated by a transformer (400kVA) and was applied on the electrodes in the vacuum interrupter. The static electrode was grounded. A limiting resistance R_L of 100 kΩ was applied in the main circuit. A voltage divider and a Pearson coil were used to measure the value of the PFV and its current, respectively. Photos of the BD process in spark conditioning were recorded by a high-speed camera. The recording rate of the camera was 580,000 frames/s and the exposure time was set at 1.285 μs.

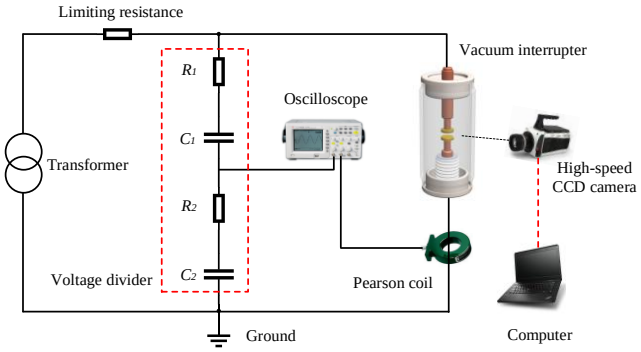

FIGURE 2 Experimental system setup of the spark conditioning under the PFV.

Table I displays the details of the experimental arrangements. The length of the electrode gap was set at 2.0 mm. The virtual values of the applied PFV ranged from 14 kV to 30 kV, which were divided into 6 grades. In order to prevent the over conditioning, the duration of the applied PFV was 20 s at each grade voltages.

Table 1. Experimental arrangements

Length of electrode gap	Applied PFVs	Duration of the applied voltage
2.0 mm	14 kV 18 kV 20 kV 24 kV 28 kV 30 kV	20 s

2.3 | Determining Method of the Pre-BD Sites in Spark Conditioning

Fig. 3 shows a planform of the multi-angle optical path system for the determination of the pre-BD sites in spark conditioning for vacuum interrupter. To determination the site, the photos of the pre-BD should be recorded at two different viewing angles at least. Through the multi-angle optical path system, the photos of the pre-BD at two viewing angles were recorded by one camera at same time. As shown in Fig. 3, there were two optical paths designed by a combination of four mirrors. By two left mirrors, the Optical path_1 made the view of the pre-BD at Viewing angle_1 appear in the left half-view of the high-speed camera. Then, through the Optical path_2, the view of the pre-BD at Viewing angle_2 should appear in the other right half-view of the camera. The angle between the two viewing angles was set at 90°. Thus, the pre-BD at two viewing angles could be recorded in one

photo at same time.

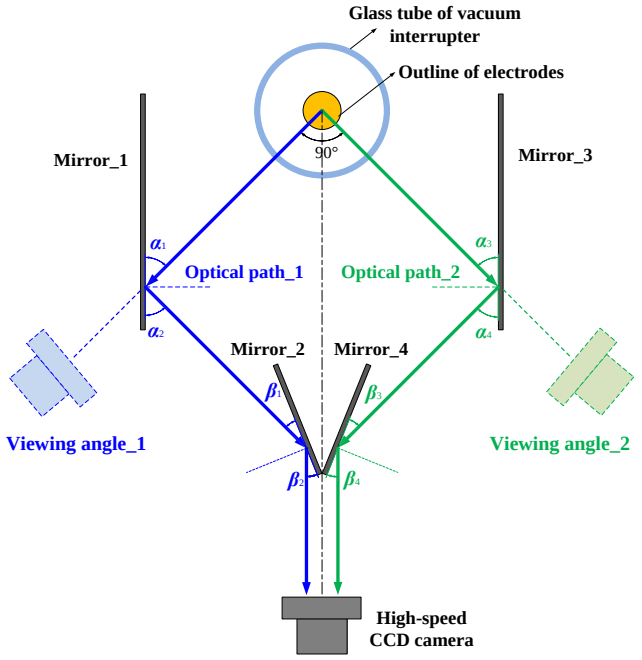

FIGURE 3 Planform of the multi-angle optical path system (top view).

Fig. 4 displays the schematic diagram of the determining method for the pre-BD sites. As shown in Fig.4, based on the photo of the pre-BD at Viewing angle_1, the length d_1, defined as the length from the axis of the vacuum spark of the pre-BD to the axis of the electrodes, could be determined quantitatively. On the same way, the length d_2 at Viewing angle_2 could be determined. Thus, the intersection of the two straight lines, according by d_1 and d_2, was regarded as the center site of the pre-BD. Based on the method above, the site of the pre-BD could be determined accurately.

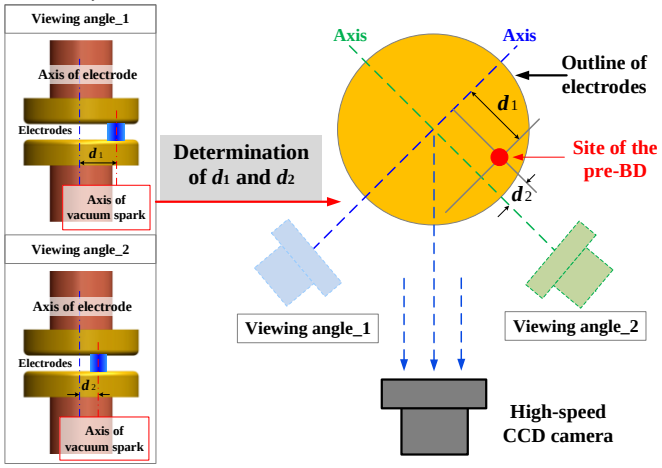

FIGURE 4 Schematic diagram of the determining method for the pre-BD sites. (top view).

3 | EXPERIMENTAL SETUP

3.1 | The Characteristics of the Pre-BD in Spark Conditioning under PFV

In this section, transient characteristics of the pre-BD in spark conditioning were investigated, which includes the voltage and current waveforms and the photos of vacuum spark in pre-BD process. The virtual value of the applied PFV was 24 kV, with the duration of 20 s.

Fig. 5 shows the typical waveforms of voltage and current during the spark conditioning under the PFV in vacuum. As displayed in Fig. 5, a large number of pre-BDs occurred in the spark conditioning process. In the duration of the applied PFV of 20 s, the pre-BDs occurred continuously in around 40 ms. The pre-BDs took place 19 times in total and were labelled by the serial numbers. In each time of pre-BDs, the voltage dipped suddenly and then recovered rapidly. The peak vale of current of the pre-BDs ranged from 1.4 to 7.2 A. The 19 times of the pre-BD distributed unevenly in four half waves of the PFV.

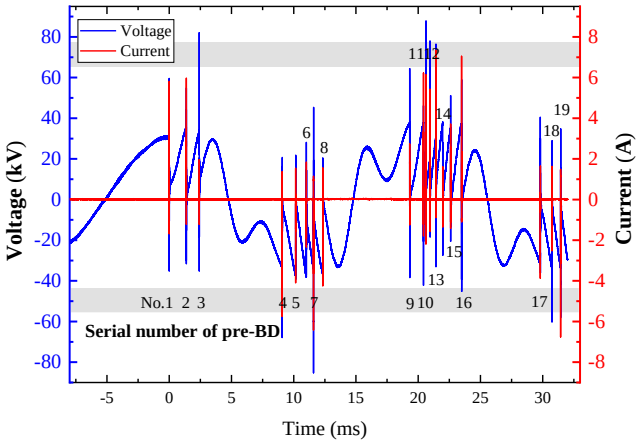

FIGURE 5 Typical voltage and current waveforms of the 19 times pre-BDs in the spark conditioning under PFV of 24 kV.

To understand the transient characteristics of the pre-BD in spark conditioning under PFV in detail, Fig. 6 displays the waveforms of the voltage and current in No.1 pre-BD. As shown in Fig. 6, in No.1 pre-BD process, the voltage dipped suddenly to zero at the value of 30.5 kV, with great oscillations. The current increased rapidly with a peak value of 5.8 A. The oscillation of the current sustained 5.1 μs. The duration of the voltage oscillation sustained 19.2 μs.

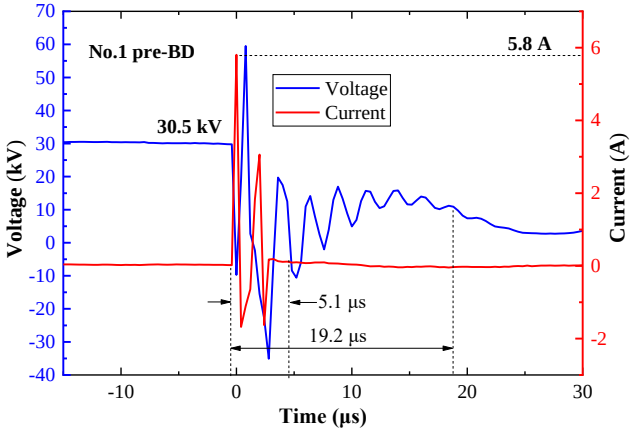

FIGURE 6 Details of the voltage and current waveforms in the No.1 pre-BD during spark conditioning under PFV of 24 kV.

Fig. 7 displays the photos of the vacuum spark in the No.1 pre-BD during spark conditioning under PFV of 24 kV,

corresponding to the waveforms in Fig. 6. Yellow solid lines labelled the outline of electrodes. The time labeled in Fig. 7 is consistent with that in Fig. 6. In each photo, there are two views of the vacuum spark of the pre-BD. The left part view is the vacuum spark of the pre-BD that observed at Viewing angle_1. The right part view is the vacuum spark of the pre-BD that observed at Viewing angle_2.

As shown in Fig.7, in each time pre-BD, the bright vacuum spark could be observed and recorded. The time between the two adjacent photos was 1.7 μs. Based on the photos of the vacuum spark, the duration of the No.1 pre-BD process at least continued for 5.1 μs. In the first recorded photo, at t=-0.4 μs, a bright vacuum spark suddenly appeared in the space between the electrodes. One frame later, at t=1.3 μs, the light intensity of the vacuum spark strengthened. However, the site of the vacuum spark fixed. After the next frame, at t=3.0 μs, the light intensity of the vacuum spark decayed significantly, with only a small bright spot remained in the pre-BD site. In the last frame, at t=4.7 μs, the light intensity of the vacuum spark decayed further, which corresponding to the decay of the current waveform in Fig. 6.

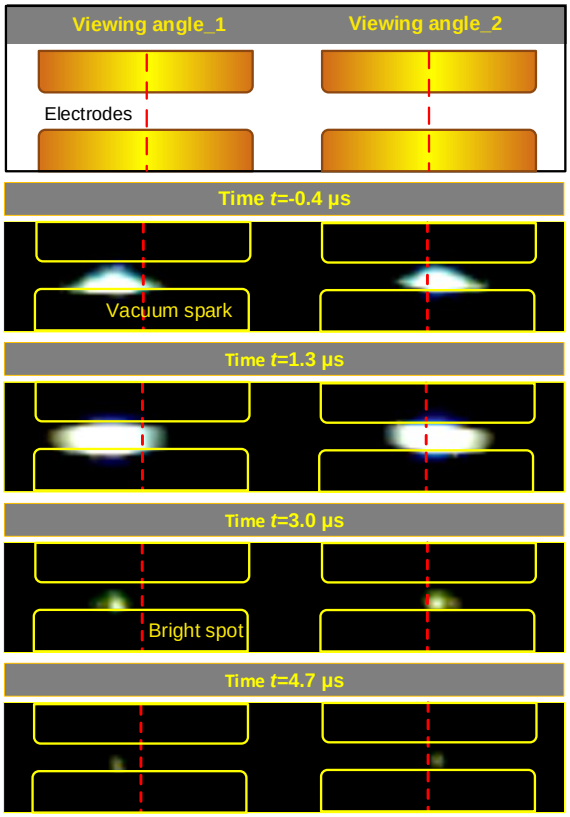

FIGURE 7 The photos of vacuum spark in the No.1 pre-BD during spark conditioning under PFV of 24 kV.

The results show that, in the spark conditioning under PFV, there were a number of pre-BDs occurred continuously at a random time. In one pre-BD, the duration of the vacuum spark would last for several microseconds. The peak value of the pre-BD current would reach several amperes. In the whole vacuum spark process of one pre-BD, the site of the vacuum spark remained in one spot.

3.2 | The Determination of Pre-BD Sites in Conditioning Process under PFV

In this section, the pre-BD sites in spark conditioning under PFV of 24kV were determined experimentally. The photos of the 19 times pre-BD were displayed in sequence. Based on these photos, corresponding to the waveforms of the voltage and current in Fig. 5, the pre-BD sites could be determined accurately.

Fig. 8 shows the photos of the 19 times pre-BD in conditioning at two viewing angles. Yellow solid lines were used to label the outline of electrodes. In every pre-BD process, the photos of the vacuum spark with highest intensity were chose to determine the pre-BD site. There were two views of the pre-BD spark in each photo, labelled by Viewing angle_1 and Viewing angle_2, respectively. The time of the selected photos and the duration of each pre-BD process Δt, consistent with that in Fig. 5, was labelled above of the photos.

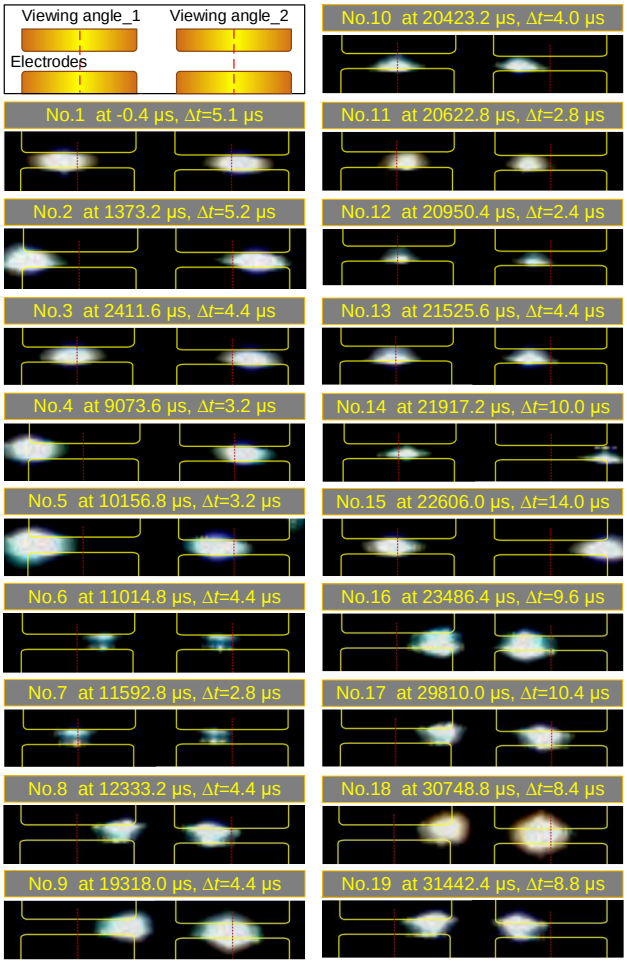

FIGURE 8 The photos of vacuum spark in 19 times pre-BD in conditioning at different viewing angles under the PFV of 24 kV.

As shown in Fig. 8, the sites of the vacuum spark in 19 times pre-BD were stochastic. There were much difference in the duration Δt in 19 times pre-BD. The minimum duration of the pre-BD Δt was 2.4 μs. The maximum duration Δt lasted 14.0 μs, took place at time of 22606.0 μs. In different pre-BDs, the intensity of the vacuum spark was quite different. In No.6 and No.7 pre-BDs, the intensity of the vacuum spark was much less than that in other pre-BDs. In No.15 pre-BD, in which the

duration Δt was the maximum of 14.0 μs, the intensity of the vacuum spark was not the highest.

Fig. 9 displays the planform of the pre-BD sites in the conditioning process under the PFV of 24 kV, based on the photos of vacuum spark in 19 times pre-BD in Fig. 8. The two viewing angles were labelled, respectively. The sites of the pre-BD were numbered in sequence, corresponding to the waveforms in Fig. 5 and the photos in Fig. 8. As shown in Fig. 9, the sites of the 19 times pre-BD randomly distributed in the whole surface of the electrodes. There was no apparent constriction of the pre-BD sites in the conditioning process under the PFV of 24 kV. The pre-BD did not repeat itself in the same place. The number of the pre-BDs appeared at the edge of the electrodes tent to be more.

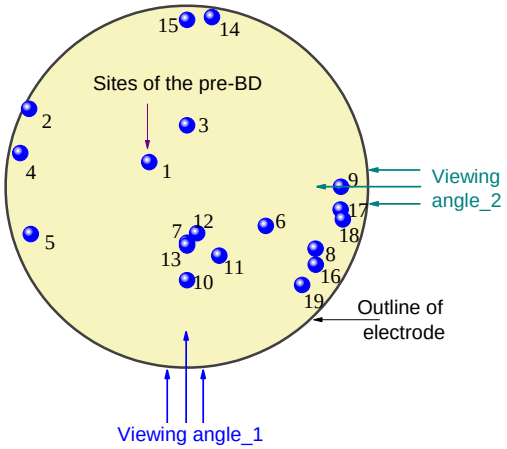

FIGURE 9 Planform of the pre-BD sites in spark conditioning process under PFV of 24 kV.

Based on Fig. 8 and Fig. 9, it can be concluded that, based on the multi-angle optical path system, the sites of the pre-BD under PFV in spark conditioning could be determined quantitatively. The experimental results indicate that there were much difference in the duration and intensity of the vacuum sparks in different pre-BDs. The sites of the pre-BD randomly distributed in the whole surface of the electrodes, without apparent constriction and did not repeat itself in the same place. The number of the pre-BDs appeared at the edge of the electrodes tent to be more.

3.3 | Distribution Characteristics of Pre-BD Sites in Spark Conditioning under PFV

In this section, the distribution characteristics and the sequential relationship of the pre-BD sites in spark conditioning under PFV are determined experimentally. The virtual value of the applied voltage increased from 14 to 30 kV. The applied duration of the PFV was 20 s.

Fig. 10 displays the distribution of the pre-BD sites in spark conditioning under various PFVs. Table 2 lists the numbers of the pre-BDs occurred under various PFVs. As shown in Fig. 10 and Table 2, under the PFV of 14 kV, there are 15 times pre-BDs occurred between the electrodes. The sites of the pre-BD located in the whole electrode surface without a clear pattern. When the PFV increased to 18 kV, the distribution of the pre-BD sites was irregular. The number of the pre-BDs increased to 17 times. When the applied PFV continuously increased to 21 kV, 24 kV and 28 kV, except for that the number of the pre-BDs increased to 20, 19 and 35 times, the distribution of the pre-BD sites located randomly in the electrode surface, without a clear pattern yet. At the 30 kV, the sites of the pre-BD almost covered the whole surface of the electrode, with a significant increase of the pre-BD number of 90 times.

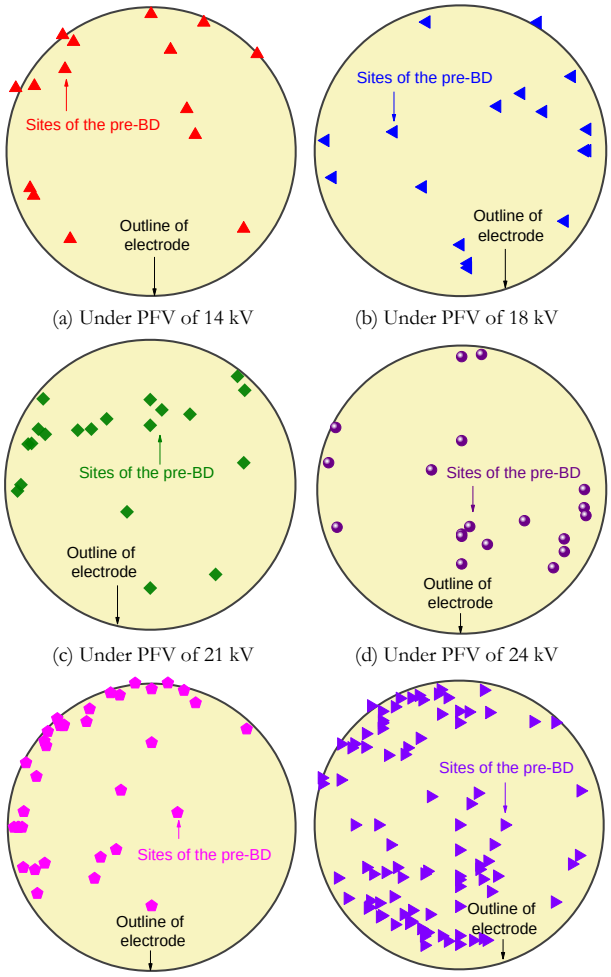

FIGURE 10 The distribution of pre-BD sites in conditioning process under various PFVs.

Table 2. Numbers of pre-BD under various PFVs

Lengths of electrode gaps	Applied PFVs	Numbers of pre-BD
2.0 mm	14 kV	15
	18 kV	17
	20 kV	20
	24 kV	19
	28 kV	35
	30 kV	90

Fig.11 displays the distribution of the total pre-BD sites under the total six PFVs. As shown in Fig. 11, the electrode surface was divided into five regions starting from the center to the edge. These regions were labeled from Region 1 to Region 5, labelled by the red solid lines, respectively. Region 1 was a circle with a diameter of 2 mm. The radius values of adjacent circles differed by 2.0 mm. In Fig. 11, under six PFVs from 14 to 30kV, the total sites of the pre-BD almost covered the whole surface of the electrode. Under six PFVs, there was no apparent constriction of the

pre-BD sites. The pre-BD sites randomly distributed in the surface of the electrode. The pre-BD did not take place twice in the same place.

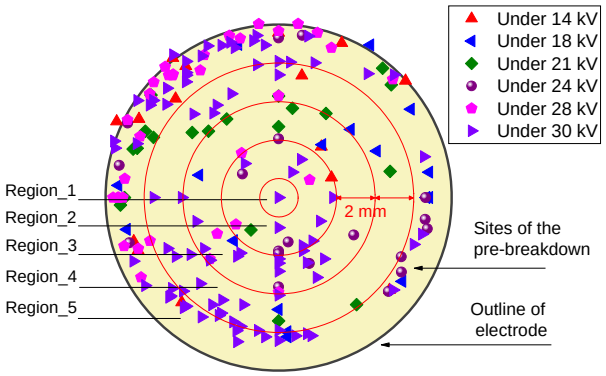

FIGURE 11 The distribution of the total pre-BD sites under six PFVs.

Table 3 displays the statistics of the pre-BD sites in the spark conditioning in the five regions under six applied PFVs. From Region_1 to Region_4, there was no clear pattern in the change of the pre-BD sites numbers. The number of the pre-BDs in Region_5 tent to be more.

Table 3. Statistics of the pre-BD sites in the spark conditioning in the five regions

Number of Region	Numbers of pre-BD under six applied PFVs					
	14 kV	18 kV	21 kV	24 kV	28 kV	30 kV
Region 1	0	0	0	0	0	1
Region 2	1	0	1	4	2	8
Region 3	1	3	3	4	4	12
Region 4	1	3	7	0	1	23
Region 5	12	11	9	11	28	46

Fig. 12 shows the numbers of pre-BD sites per square millimeter in the spark conditioning in five regions of the electrode surface. As shown in Fig. 12, under the voltage of 14 kV and 18 kV, the number of pre-BD sites per square millimeter in Region_5 was the maximum, which were 0.12 and 0.11 times per square millimeter. When the voltage increased to 21 kV and 24 kV, the maximum appeared in Region_3 and Rigion_2, which were 0.1 and 0.16 times per square millimeter. Under 28 kV, the maximum was 0.26, in Region_3. When the voltage increased to 30 kV, the number of pre-BD sites per square millimeter in the five regions ranged from 0.24 to 0.46 times per square millimeter. From Region_1 to Region_4, there was small difference in the numbers of the pre-BD sites per square millimeter.

Fig. 13 shows the sequential relationship of the 90 times pre-BD sites in the conditioning process under PFV of 30 kV. From Fig. 13(a) to Fig. 13(f), there are fifteen sites of the pre-BD in every figures. The 90 times pre-BD sites were numbered in sequence. The electrode surface was divided into four areas by two crossed solid lines, labelled from Area_1 to Area_4. As shown in Fig. 13(a), the first pre-BD occurred in Area_1. Then the second and third pre-BDs occurred in Area_2 and Area_4. In the first 15 times pre-BD, two sequential pre-BDs occurred in different site, which were hardly adjacent. In Fig. 3(b), in the 15 times pre-BD from No.15 to No.30, the sites almost located in Area_1. However, the sites of the two sequential pre-BDs were adjacent. From No.31 to No.90, as shown from Fig. 13(c) to Fig. 13(f), the pre-BD sites occurred in the same rule in the time sequence, in which the two sequential pre-BDs occurred almost in different sites and far away from each other in the electrode surface.

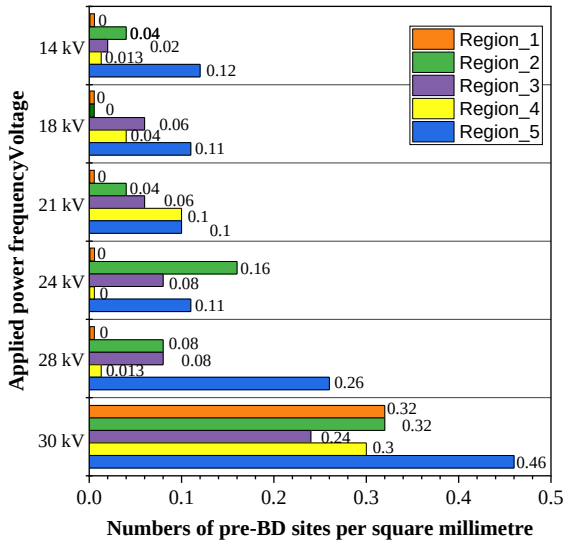

FIGURE 12 Numbers of Pre-BD sites per square millimeter in the spark conditioning in five regions of the electrode surface.

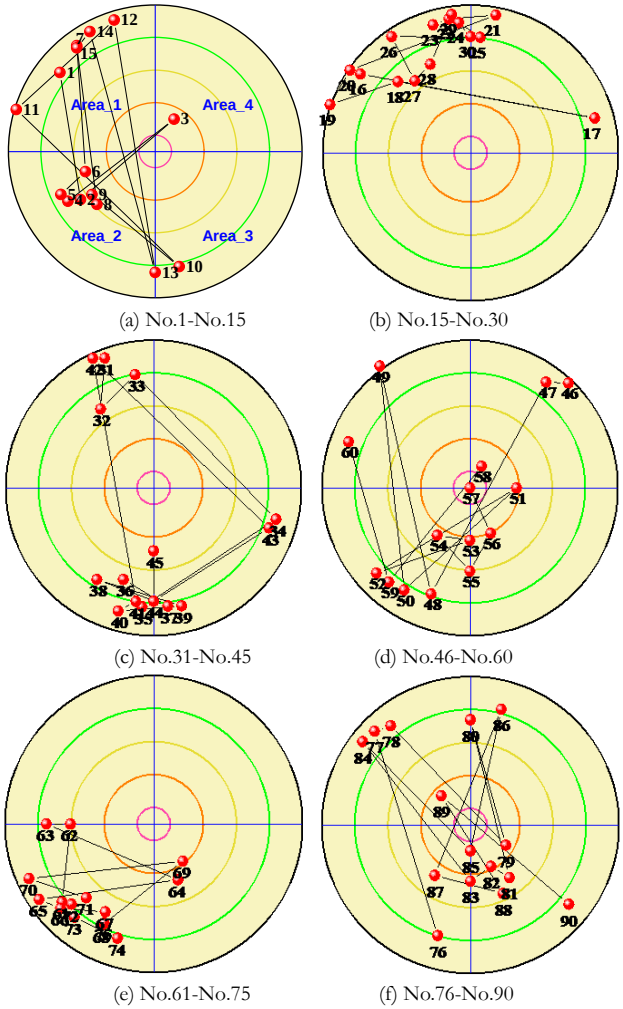

(a) No.1-No.15 (b) No.15-No.30

(c) No.31-No.45 (d) No.46-No.60

(e) No.61-No.75 (f) No.76-No.90

FIGURE 13 Sequential relationship of the 90 times pre-BD sites in spark conditioning under PFV of 30 kV.

As indicated in Fig. 10, 11 and 12, it can be concluded that, under six PFVs, the pre-BD sites randomly distributed in the surface of the electrode and almost covered the whole surface of the electrode. The number of the pre-BDs in edge region of the electrode tent to be more. Moreover, in the aspect of the time sequence, the two sequential pre-BDs occurred almost in different sites and far away from each other in the electrode surface. Thus, the pre-BDs took place independently in both time and space, in which there should be no effect between each other of two sequential pre-BDs.

4 | DISCUSSION

4.1 | The Role of The Pre-BD for Electrode Surface in Spark Conditioning Process under PFV

In this paper, the transient characteristics of the pre-BD in spark conditioning under PFV was determined. As shown in Fig. 5, under the application of PFV at a certain value, a number of pre-BDs occurred continuously at a random time. Fig. 6 and Fig. 7 indicate that the pre-BD would last for several microseconds and the peak value of the current would reach several amperes. Fig. 11 and Fig. 13 reveal that the pre-BDs in conditioning under the PFV would be independent in both time and space, which would take place all over the electrode surface irregularly. Therefore, under the spark conditioning of PFV, the surface of electrode was reated mainly through the vacuum sparks of number times of pre-BDs. In each times of pre-BD, the micro-protrusion and the defects in one site of the electrode surface should be removed.

Comparing to the role of the LIV for electrode surface in conditioning process [14, 16, 24], there are two differences for that under the PFV. Firstly, the duration of the discharge process in conditioning is different. Under the LIV, the duration of the discharge process would reach several tens microseconds [22]. Under the PFV, the duration of one pre-BD would last for only several microseconds. Secondly, the number of discharges in conditioning is different. Under the LIV, there was only one discharge in each time of conditioning after the application of high voltage. Under the PFV, the pre-BD would take places large number of times after the application of the high voltage. Moreover, in the two adjacent pre-BDs, the discharge processes are independent of each other. Thus, in the one time of application of the PFV, the defects in large numbers of sites in the electrode surface should be removed. As a conclusion, the efficiency of the conditioning under the PFV should be higher than that under the lightning impact voltage.

4.2 | Effect of the Electric Field on Pre-BD Sites in Conditioning under PFV

To investigate the effect of the electric field on the pre-BD sites in conditioning process under PFV, an electrostatic field calculation model was built according the experimental setting. Fig.14 displays the distribution of the electric field between the electrodes under the experimental voltage of 30 kV. As shown in Fig.14, the electric field between the electrodes distributed uniformly in regions from No.1 to No.4. In these regions, the electric field intensity maintained around 1.50×10^7 V/m. In the edge region of No.5 and the filleting area of the electrode, the electric field intensity strengthened to 1.77×10^7 V/m.

As displayed in Fig.11 and Table 3, the distribution of the total pre-BD sites under six PFVs reveal that the pre-BD sites randomly distributed in the surface of the electrode, in which the number of the pre-BDs in Region_5 tent to be more. As revealed in Fig. 12, under a certain applied voltage, there was no significant difference in the numbers of pre-BD sites per square millimeter in the spark conditioning, in the regions from Region_1 to Region_4. However, the number of pre-BD sites per square millimeter in the Region_5 should be obviously higher than that in other four regions. This phenomena could be explained in two aspects. Firstly, the distribution of the pre-BD sites should be effected by the electric field intensity between the electrodes. As displayed in Fig.14, the distribution law of the experimental pre-BD sites was in accordance with the electric field between the electrodes. In edge region of Region_5, in which there was a higher electric field, the pre-BD should occur more frequently, which is the same as that in the case of the BD site in the conditioning under the LIV[22]. Secondly, the distribution of the pre-BD sites should be effected by the micro-surface condition of different regions in electrode surface. In the processing of the electrode, the edge region should be chamfered, leading to more particles and defects in this region.

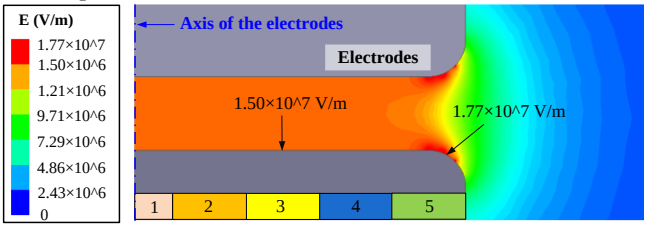

FIGURE 14 Distribution of the electric field between the electrodes under experimental voltage of 30 kV.

4.3 | Physical Mechanism of Pre-BD in Conditioning Process under PFV

In this paper, the transient characteristics of the pre-BD in spark conditioning could be revealed by the photos of the vacuum spark in Fig. 7 and the waveforms of the 19 times pre-BD in conditioning in Fig. 8. Based on the experimental results, it could be concluded that, what matters in conditioning process under PFV should be the large numbers of the pre-BDs. Thus, the effect of a single pre-BD on the treatment of the electrode surface and the numbers of the pre-BDs under a certain voltage should be the keys in the understanding of the physical mechanism in conditioning process of the electrodes under FPV. Moreover, as revealed in Fig. 13, the two sequential pre-BDs occurred almost in different sites and far away from each other in the electrode surface. As a result, in the conditioning under PFV, the pre-BDs took place independently, in which there should be no effect between each other of two sequential pre-BDs.

Therefore, as shown in Fig. 15, under the application of PFV, the physical mechanism of the pre-BD on the treatment of electrode surface in conditioning process could be divided in four stages. 1) **Stage_1**, formation of the high electric field stage: Under the application of PFV, an extra-high electric field region should form at the tip of one of the micro protrusions. 2) **Stage_2**, formation of the molten drop stage: Under the extra-high electric field and the field emission, the top of this micro protrusion started to melt. A molten drop formed at the top of this micro

protrusion. Under the continues heating, the molten drop started to explode and vaporize. 3) **Stage_3**, formation of conducting channel stage: Under the particle collisions and the electron impact in metal vapor, the metal vapor was turned to metal plasma. Then, an electric channel was built between the electrode and the current started to flow. 4) **Stage_4,** extinguishment of the pre-BD vacuum spark stage: as the disappear of the micro protrusions, there was no enough sustained energy for the maintenance of the plasma. The plasma diffused to the space between electrode and vacuum spark of the pre-BD extinguished. As a result, after the tip of the micro protrusion disappeared, there was no source of the metal vapor and plasma. Therefore, the pre-BD could not maintain and rapidly extinguished in several microseconds. This understanding could provide an explanation for independent phenomena of the two sequential pre-BDs in the conditioning under PFV.

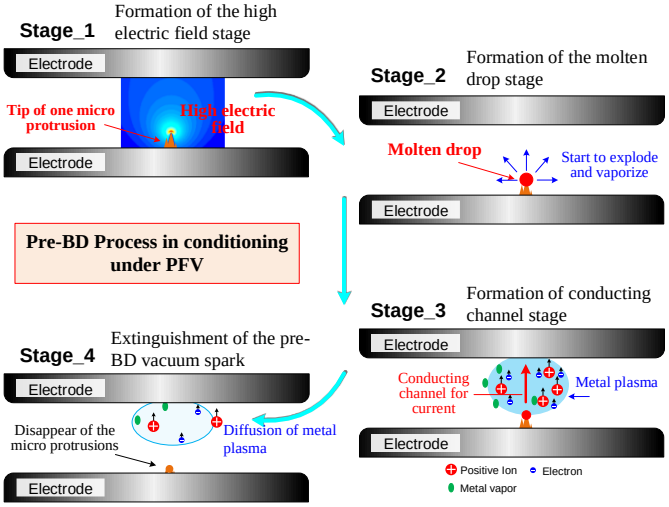

FIGURE 15 Schematic diagram of the physical mechanism of the pre-BD in conditioning process under the application of PFV.

5 | CONCLUSION

In this paper, the transient characteristics and sites of the pre-BD in the spark conditioning under PFV in vacuum has been determined experimentally. The following conclusions can be drawn.

1. In the spark conditioning under PFV of vacuum interrupters, the pre-BDs continuously occurred at a random moment. Within several half-waves, the number of the pre-BDs could reach dozens of times, which was the key for the treatment of the electrode surface in conditioning.
2. Under the application of PFV, the single pre-BD occurred at a random moment, in which would last for several microseconds and the peak value of the current would reach several amperes. Under PFV of 24 kV, the peak value of the current in pre-BDS would reach 7.2 A and the vacuum spark always stayed in one site and sustained from 2.4 to 14.0 μs.
3. Under six PFVs, there was no apparent constriction of the pre-BD sites. The pre-BD sites randomly distributed in the surface of the electrode and almost covered the whole surface of the electrode. The number of the pre-BDs in edge region of the electrode tent to be more.
4. The two sequential pre-BDs occurred almost in different sites and far away from each other in the electrode surface. The pre-BDs took place independently in both time and space, in which there should be no effect between each other of two sequential pre-BDs.

REFERENCES

[1] P. G. Slade, "The Vacuum Interrupter Theory, Design, and Application," pp. 72-88, Boca Raton: CRC Press, 2008.
[2] A. De Lorenzi, M. Kashiwagi, H. P. L. De Esch, N. Pilan, A. Kojima, L. Svensson, G. Chitarin, N. Umeda, and H. Tobari, "HV holding in vacuum, a key issue for the ITER neutral beam injector, " *Proceedings - International Symposium on Discharges and Electrical Insulation in Vacuum*, pp. 721-725, 2018.
[3] R. V. Latham, "High Voltage Vacuum Insulation: Basic Concepts and Technological Practice", London: academic Press Inc, 1995.
[4] Y. Fukuoka, T. Yasuoka, K. Kato, and H. Okubo, "Breakdown conditioning characteristics of long gap electrodes in a vacuum," *IEEE Transactions on Dielectrics and Electrical Insulation,* vol. 14, no. 3, pp. 577-582, Jun, 2007.
[5] F. Miyazaki, Y. Inagawa, K. Kato, M. Sakaki, H. Ichikawa, and H. Okubo, "Electrode conditioning characteristics in vacuum under impulse voltage application in non-uniform electric field," *IEEE Transactions on Dielectrics and Electrical Insulation,* vol. 12, no. 1, pp. 17-23, Feb, 2005.
[6] C. C. Erven, Vanheesw.Rg, and K. D. Srivastava, "60 HZ behavior of vacuum insulation in high-voltage switchgear," *IEEE Transactions on Power Apparatus and Systems,* vol. PA91, no. 4, pp. 1589-1595, 1972.
[7] Y. Zhang, Z. Liu, S. Cheng, L. Yang, Y. Geng, and J. Wang, "Influence of Contact Contour on Breakdown Behavior in Vacuum under Uniform Field," *IEEE Transactions on Dielectrics and Electrical Insulation,* vol. 16, no. 6, pp. 1717-1723, Dec, 2009.
[8] T. Lamara, "Vacuum Contacts Conditioning by a Glow Argon Discharge Using AC Power Source," *IEEE Transactions on Plasma Science,* vol. 39, no. 11, pp. 2586-2587, Nov, 2011.
[9] J. D. Cross, and B. Mazurek, "Fast cathode processes in conditioning of vacuum electrodes," *IEEE Transactions on Electrical Insulation,* vol. 23, no. 1, pp. 87-89, Feb, 1988.
[10] T. Shioiri, T. Kamikawaji, E. Kaneko, M. Homma, H. Takahashi, and I. Ohshima, "Influence of electrode area on the conditioning effect in vacuum," *IEEE Transactions on Dielectrics and Electrical Insulation,* vol. 2, no. 2, pp. 317-320, Apr, 1995.
[11] . Okubo, F. Miyazaki, Y. Inagawa, K. Kato, M. Sakaki, H. Ichikawa, "Electrode area of breakdown depending on - Conditioning mechanism under non-uniform electric field in vacuum," *ISDEIV: XXIth International Symposium on Discharges and Electrical Insulation in Vacuum, Vols 1 and 2, Proceedings*, pp. 76-79, 2004.
[12] K. Kato, T. Yasuoka, Y. Fukuoka, H. Saitoh, M. Sakaki, and H. Okubo, "Investigation of electrode conditioning mechanism in vacuum with impulse voltage application, " *ISDEIV: XXIth International Symposium on Discharges and Electrical Insulation in Vacuum, Vols 1 and 2, Proceedings*, 2006.
[13] A. V. Schneider, E. L. Dubrovskaya, S. A. Onischenko, "The Effect of High-Frequency Arc Conditioning of the Electrodes on Electric Strength of Vacuum Insulation," *International Symposium on Discharges and Electrical Insulation in a Vacuum.* pp. 81-84, 2018.
[14] H. Kojima, N. Hayakawa, R. Nishimura, H. Okubo, H. Sato, H. Saito, and Y. Noda, "Conditioning Mechanism of Cu-Cr Electrode Based on Electrode Surface State under Impulse Voltage Application in Vacuum," *IEEE Transactions on Dielectrics and Electrical Insulation,* vol. 18, no. 6, pp. 2108-2114, Dec, 2011.
[15] H. Kojima, T. Takahashi, N. Hayakawa, K. Hasegawa, H. Saito, and M. Sakaki, "Dependence of Spark Conditioning on Breakdown Charge and Electrode Material under a Non-Uniform Electric Field in Vacuum," *IEEE Transactions on Dielectrics and Electrical Insulation,* vol. 23, no. 5, pp. 3224-3230, Oct, 2016.
[16] H. Kojima, T. Takahashi, N. Hayakawa, K. Hasegawa, and M. Sakaki, "Optimum Breakdown Charge for Maximum Dielectric Strength in Spark Conditioning in Vacuum under a Non-uniform Electric Field," *IEEE Transactions on Dielectrics and Electrical Insulation,* vol. 24, no. 4, pp. 2660-2665, Aug, 2017.
[17] T. C. Balachandra, and G. R. Nagabhushana, "Anode hotspot temperature estimation in vacuum gaps under 50 hz alternating excitations," *IEEE Transactions on Electrical Insulation,* vol. 28, no. 3, pp. 392-401, Jun, 1993.
[18] L. Yang, Y. Feng, W. Zhang, J. Wang, and Y. Qiu, "Study on spark conditioning of vacuum switch with a parallel capacitor," in Eleventh International Symposium on High Voltage Engineering, 1999, pp. 368-71 vol.3.

[19] N. S. Xu, and R. V. Latham, "Electrical and spatial correlations between direct-current prebreakdown electron-emission characteristics and subsequent breakdown events," *Journal of Physics D-Applied Physics,* vol. 27, no. 12, pp. 2547-2555, Dec 14, 1994.

[20] R. V. Latham, K. H. Bayliss, and B. M. Cox, "Spatially correlated breakdown events initiated by field electron-emission in vacuum and high-pressure SF_6," *Journal of Physics D-Applied Physics,* vol. 19, no. 2, pp. 219-231, Feb 14, 1986.

[21] S. Kobayashi, N. S. Xu, Y. Saito, R. V. Latham "Distributions of prebreakdown emission sites on broad area rounded shaped copper cathode of a vacuum gap," *Isdeiv: Xviiith International Symposium on Discharges and Electrical Insulation in Vacuum - Proceedings, Vols 1 and 2*, pp. 56-59, 1998.

[22] Y. Du *et al.*, Distribution of Breakdown Positions in Conditioning Progress Between Plane-Plane Electrodes in Vacuum Under Lightning Impulse Voltage, *The Proceedings of the 16th Annual Conference of China Electrotechnical Society. Lecture Notes in Electrical Engineering,* 2022, pp. 179-87.

[23] M. Xiangteng *et al.*, *Effect of Limiting Resistance on Distribution of Breakdown Positions under Lightning Impulse Voltage between Sphere-Plane Electrodes in Vacuum*, IEEE International Conference on High Voltage Engineering and Application. 2020, pp. 4 pp.-4 pp.

[24] H. Ma, G. Li, Z. Liu, Y. Geng, J. Wang, and H. Kojima, "Reshaping of Micro-morphology Feature in Electrode Surface under Conditioning by Lightning Impulse Voltage in Vacuum Gaps," *IEEE Transactions on Dielectrics and Electrical Insulation,* vol. 27, no. 6, pp. 2056-2063, Dec 2020.